# Upgrades to the NIST/DARPA EUV Reflectometry Facility

C. Tarrio, T. B. Lucatorto, S. Grantham, M. B. Squires, U. Arp, and L. Deng
Electron and Optical Physics Division, National Institute of Standards and Technology
Gaithersburg, MD, 20899-8410, USA

We have recently installed a new sample chamber at the NIST/DARPA EUV Reflectometry Facility at the National Institute of Standards and Technology. The chamber replaces a much smaller system on Beamline 7 at the Synchrotron Ultraviolet Radiation Facility that was commissioned almost ten years ago as a dedicated facility for the measurement of normal-incidence extreme ultraviolet optics used in lithography development, astronomy, and plasma physics. The previous measurement chamber was limited to optics less than 10 cm in diameter, and, thus, we were not able to measure many of the optics used in modern telescopes and extreme ultraviolet lithography steppers. The new chamber was designed to accommodate optics up to 36 cm in diameter and weighing up to 40 kg, and with modifications will be able to measure optics up to 50 cm in diameter. It has three translation and three rotation axes for the sample and two rotation axes for the detector, with an accuracy of better than 0.5 mm in translation and $0.04^{o}$ in rotation. We will describe design considerations, performance of the positioning mechanisms, and initial reflectivity measurements of both curved and flat surfaces.

**Keywords**: Extreme ultraviolet; metrology; reflectometry; lithography

## 1. Introduction

The NIST/DARPA National EUV Reflectometry Facility was commissioned in 1993 to serve the growing community of researchers in need of absolute extreme ultraviolet (EUV) mirror metrology.[1] Although researchers had been working in the EUV for decades, the development of efficient normal-incidence multilayer mirrors for the EUV accelerated the need for accurate measurements. Multilayer mirrors are used in scientific pursuits such as astronomy,[2] microscopy,[3] and plasma physics;[4] however, our facility was designed from the beginning to support the development of EUV lithography (EUVL).[5]

## 2. System design

Figure 1 is a schematic diagram of our beamline. The source of radiation for our beamline is the Synchrotron Ultraviolet Radiation Facility, or SURF III.[6] This is a single-magnet electron storage ring with an 83.8 cm radius. It can be operated reliably at energies from a few tens of MeV up to 380 MeV. This allows us to adjust the peak wavelength to minimize second-order and scattered radiation. The small bending radius allows for placement of the first collection mirror very close to the tangent point. This first mirror is a nickel-coated toroid that collects 20 mrad by 3 mrad of the emitted radiation, operating at a 3° grazing angle of incidence. The vertical collection angle was designed to subtend virtually all of the vertical emission angle for EUV radiation. The beam is imaged one-to-one on an adjustable entrance slit. A second 3° toroid directs the radiation to one of two plane, varied-line-spacing gratings: a 600 $mm^{-1}$, 5°-incidence, or 1500 $mm^{-1}$, 3.5°-incidence grating. The 5° grating is blazed for 20 nm wavelength to operate between 10 nm and 40 nm, while the 3.5° grating is blazed for 8 nm, to work between 3 nm and 15 nm. Wavelength is selected by a plane Au-coated fused silica scan mirror that rotates and translates.


Soft X-Ray and EUV Imaging Systems II, Daniel A. Tichenor, James A. Folta, Editors,
Proceedings of SPIE Vol. 4506 (2001) © 2001 SPIE · 0277-786X/01/$15.00

Downloaded From: http://proceedings.spiedigitallibrary.org/ on 01/27/2016 Terms of Use: http://spiedigitallibrary.org/ss/TermsOfUse.aspx

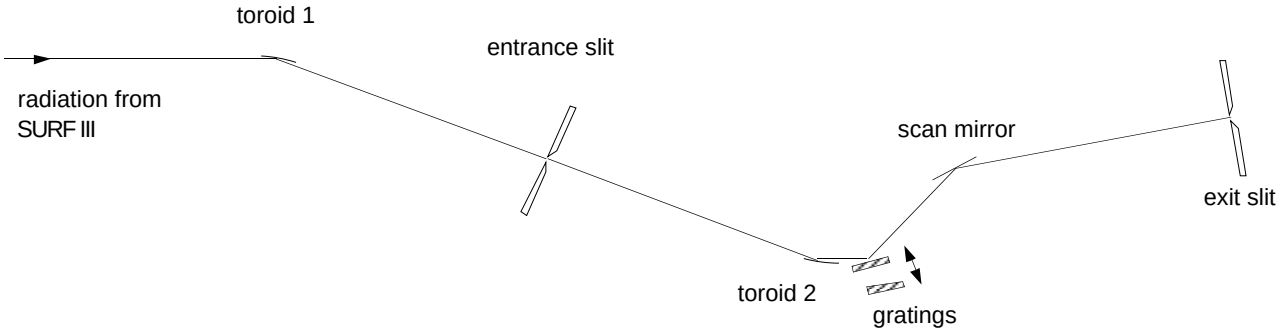


Figure 1. Optical layout of our monochromator.

The scale of the original design for the new sample chamber, done in 1993, was based upon early conceptualizations of the EUV stepper optics. At that time we expected the largest mirror in such a stepper to be less that 35 cm in diameter and of order 40 kg in mass. (We understand now that present stepper designs might have mirrors as large as 50 cm in diameter.) The recently commissioned Engineering Test Stand, or ETS, at Sandia National Laboratories, built in collaboration with Lawrence Livermore and Lawrence Berkeley National Laboratories, is the first EUV system capable of exposing large fields of view. This system has a condenser with two near-normal-incidence mirrors and two grazing reflections, and a four-mirror imaging system. The largest mirror of this system is the first condenser, or C1 optic, which is 28 cm in diameter and 7.5 cm thick at the edge. The NIST reflectometer is presently the only instrument in the world large enough to make a complete set of measurements on the intact C1 system.

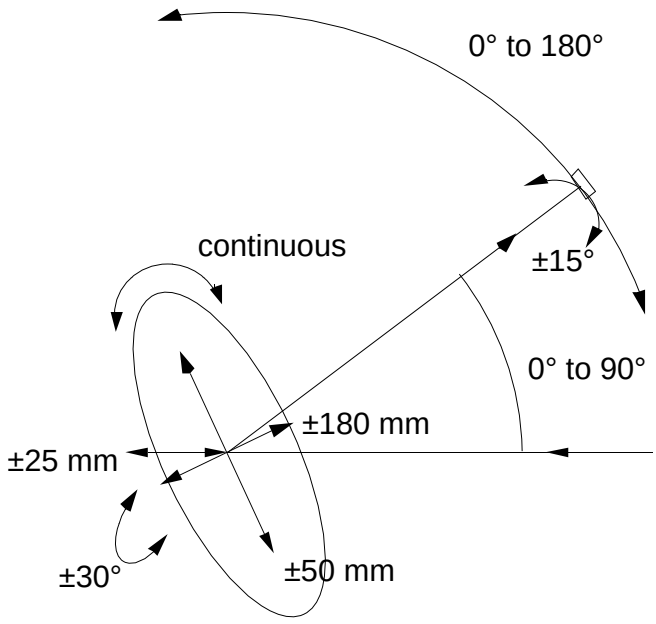


Figure 2. Schematic of sample chamber motion axes. Radiation is incident from the right.

The resulting chamber is 1.9 m in diameter and about 3 m long. It has six sample axes of motion and two detector axes. The sample angle of incidence is the first level of motion. This is done by an external motor and a pair of worm gears driving differentially pumped rotary seals. Within the vacuum system is a transverse tilt axis capable of tilting the sample ±30° about the plane of reflection. Upon this are three independent translation axes. There is 50 mm of piston motion to bring the sample face to the axis of rotation. Then there are 100 mm vertical by 360 mm horizontal translation. The final stage of motion is a continuous azimuthal rotation of the platen about its center. The combination of this with the 360 mm horizontal translation assures that we will be able to reach the entire surface of a large optic. [See Fig. 2.]

There are also two axes of detector motion. The detector arm is able to rotate 180° in the plane of reflection. Also, to change detectors or to measure very strongly curved optics, there is ±15° of motion transverse to the plane of reflection. This, coupled with the 30° of sample tilt allows us to measure optics with up to a 45° curvature, or a 0.7 numerical aperture.



Downloaded From: http://proceedings.spiedigitallibrary.org/ on 01/27/2016 Terms of Use: http://spiedigitallibrary.org/ss/TermsOfUse.aspx

# 3. System performance

The requirements of the optics in an EUV stepper put the most stringent demands on the level of performance for the reflectometer. Gullikson, *et al.*[7] have described the required metrology specifications for such optics. The ultimate requirements are: wavelength precision at 13.4 nm = 0.005%; wavelength accuracy = 0.02%; positional accuracy $0.04^0$ in angle, 0.5 mm in linear displacement; peak reflectance precision = 0.06%, accuracy = 0.1%. We describe below our ongoing approach to achieve the required level of performance.

## *3.1. Characterization of incident radiation*

Three elements are of crucial importance in achieving highly accurate reflectivity measurements: the radiation must be spectrally pure, i.e., relatively free of out-of-band radiation; and the wavelength, $\lambda$, and the intensity of the incident radiation, $I_0$, must be accurately known. Figure 3 shows the throughput of our beamline when the storage ring is operating at 285 MeV. The three traces represent photons/s for the high-energy grating with a C filter (3 nm to 14 nm), low-energy grating with Be filter (11 nm to 20 nm) and low-energy grating with Al filter (17 nm-34 nm). These measurements were made under typical operating conditions: 0.5-mm entrance slit and 0.5-mm exit slit widths, giving a resolving power ($\lambda/\delta\lambda$) of roughly 500 with the high-energy grating and 200 with the low-energy grating. The average stored current is about 200 mA, yielding an incident photon beam of order $2\times10^{11}$ $s^{-1}$ at 13 nm. With the 10-pA noise floor of our Si photodiode detector and readout electronics, this flux allows a dynamic range of $10^5$.

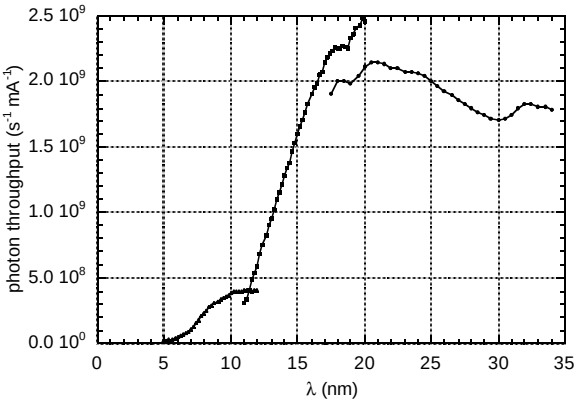


Figure 3. Beamline throughput.

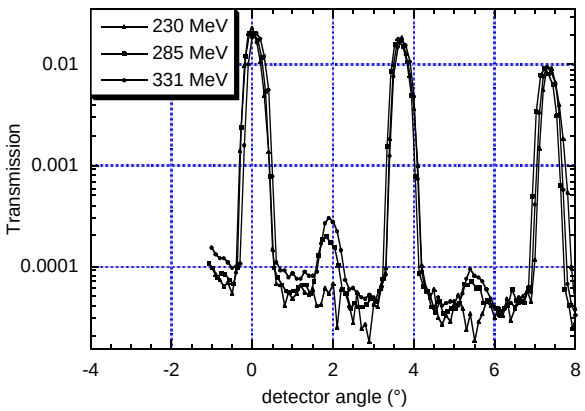


Figure 4. Detector scans measured at 13 nm for a variety of electron-beam energies.



Downloaded From: http://proceedings.spiedigitallibrary.org/ on 01/27/2016 Terms of Use: http://spiedigitallibrary.org/ss/TermsOfUse.aspx

### 3.1.1. Spectral purity

We have made some preliminary estimates of the spectral purity of our incident radiation using a 5000 $mm^{-1}$ freestanding transmission grating[8]. Using the unique versatility of SURF III that allows measurements at a variety of stored electron-beam energies, we can easily find conditions that minimize the second order component. Figure 4 shows the spectral content of the monochromator with Be filter measured when the high-energy grating is tuned to 13 nm at a variety of electron-beam energies. These data were taken with the transmission grating placed normal to the output beam and the detector scanned through the orders of the radiation diffracted by the grating. It is apparent that there is noticeable second-order radiation at 330 MeV, but none detectable at 230 MeV. At 331 MeV there is a factor of 50 more 6 nm radiation from SURF than at 230 MeV as shown in Fig. 5. Because the low-energy grating is blazed for 20 nm rather than 8 nm, similar spectral purity is obtained for a beam energy of 280 MeV. We use this configuration for most measurements.

Figure 6 shows scans of diffracted intensity vs. wavelength for two different diffraction angles, measured with the same transmission grating. These are a measure of scatter in our system. There appears to be a fairly constant background that is about a factor of 400 smaller than the diffraction peaks. However, the most telling feature of these scans is the abrupt drop in signal at 11.1 nm, the absorption edge of the 0.2 μm Be filter that we use to filter higher-order radiation and long-wavelength scatter. This drop indicates that the background at longer wavelengths is most likely due to scatter from the transmission grating rather than scatter in our monochromator. The ratio of diffraction peaks to the non-wavelength-specific signal, i.e., that below the Be absorption edge is greater than a factor of 2000.

This factor of 2000 is not necessarily an absolute measurement of scattered-light contribution to our incident radiation, however. Since the total contribution is some integration over an unknown band, we must develop some other test of the scattered-light contribution. We plan on making measurements of test samples at several beam energies and with several filter combinations in order to determine the absolute out-of-band contribution to our monochromator throughput.

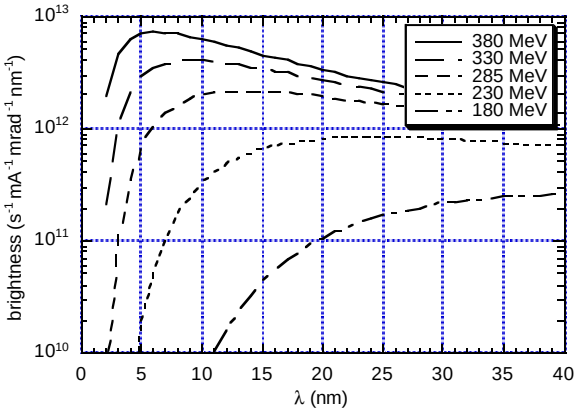


Figure 5. Spectral brightness of SURF at several primary beam energies. We collect virtually all the vertical extent of the radiation.

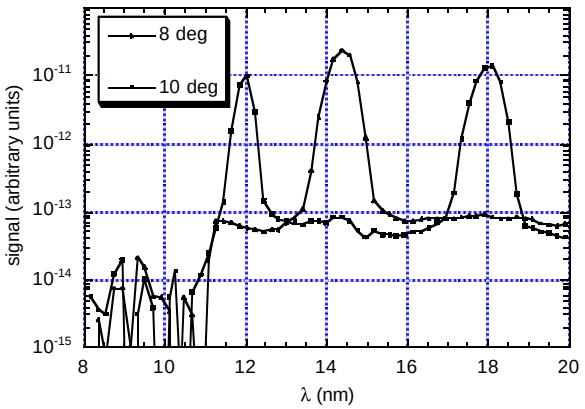


Figure 6. Diffraction through a 5000 $mm^{-1}$ transmission grating as a function of wavelength at two angles.



Downloaded From: http://proceedings.spiedigitallibrary.org/ on 01/27/2016 Terms of Use: http://spiedigitallibrary.org/ss/TermsOfUse.aspx

### 3.1.2. Measurement of incident intensity

Reflectivity measurements are made by scanning the wavelength range with the detector in the direct beam, then moving everything so that the beam hits the desired spot on the sample, then reflects at the desired angle to the detector, which has itself been moved to the appropriate location. The wavelength is then scanned again, and the ratio of the reflected to incident intensity is calculated. The absolute accuracy of these measurements depends on the spectral purity as discussed above. However drift in the beamline throughput can be present from any number of sources, the largest usually being heating of the first beamline mirror (toroid 1 in Fig. 1). Many reflectometry facilities address this problem by alternating measurements of reflectance with normalization runs. This is not practical for us: the large size of the sample chamber means that it takes several minutes to position all the internal components. Thus we have investigated several different normalization methods, and settled upon having a second exit slit, displaced 5 mm vertically (in the dispersion plane) from and with identical dimensions to the actual exit slit. There is an XUV-sensitive photodiode, identical to that used in our measurements, behind this slit, and the photocurrents from the two detectors are measured simultaneously to account for both drift and short-term fluctuations in incident intensity. Figure 7 shows the ratio of detected photocurrent behind this slit to that measured by the sample chamber diode. These data were obtained over two hours and vary by less than 0.2%. Measuring the direct beam every hour and interpolating will reduce this uncertainty component to less than 0.1%.

### 3.1.3. Calibration of wavelength

The best way to determine the wavelength is to use an atomic absorption line or metallic absorption edge to calibrate the monochromator. To determine the absolute wavelength at 13.4 nm, we periodically use a Kr absorption cell. The same double-slit scheme that enables very good normalization also allows us to use the Be K edge at 11.1 nm to calibrate the monochromator for each scan of the sample being tested. Repeated measurements of the position of the Be absorption edge measured through both slits indicate a separation of 0.50 nm. This arrangement allows us to scan through the Be edge with each separate reflectivity measurement, if necessary, without needing to move the sample.

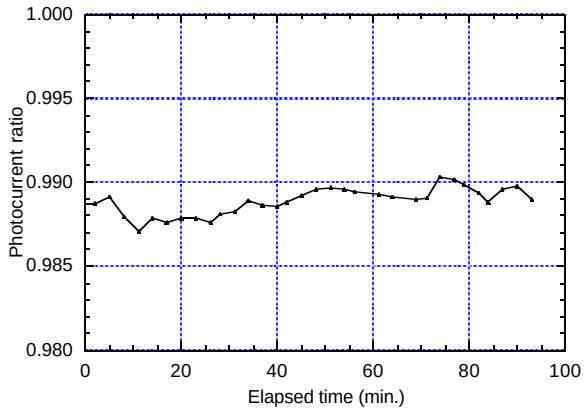


Figure 7. Ratio of photocurrent detected behind reference to that detected at the beamline detector.

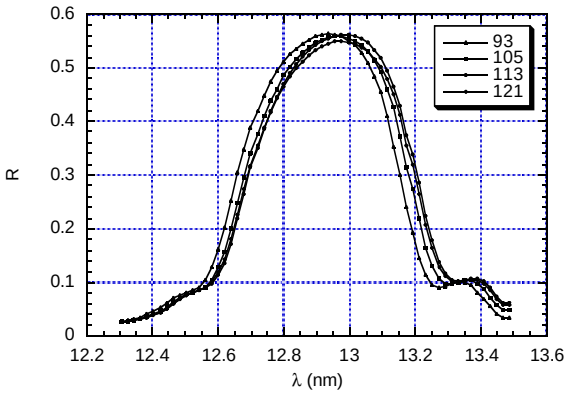


Figure 8. Reflectivity of ETS C1 optic at four radii. Radii in mm are noted in the legend.



Downloaded From: http://proceedings.spiedigitallibrary.org/ on 01/27/2016 Terms of Use: http://spiedigitallibrary.org/ss/TermsOfUse.aspx

**Table 1. Coordinate parameters for measurement of C1 optic.**

| radius (mm) | angle of incidence (°) | surface slope (°) | surface height from center of rotation (mm) |
|---|---|---|---|
| 93.0 | 20.50 | 23.82 | 20.91 |
| 105.0 | 22.98 | 26.54 | 26.55 |
| 109.0 | 23.79 | 27.43 | 28.59 |
| 121.0 | 26.16 | 30.04 | 35.18 |

### 3.1.4. Initial Results

Our first measurements of a large, curved optic were made on the C1 optic of the ETS. This is a 27-cm diameter asphere with an approximate radius of curvature of 25 cm. Measurements of slower optics can be made at constant angle of incidence, and the results modeled to account for the small differences in operating angle in the optical system. However, the differences in working angle across the surface of the C1 optic are large enough that reflectivity peak for a constant angle of incidence would shift considerably in wavelength. This would add considerable uncertainty in modeling results due to changes in optical constants of the Mo and Si over such a large wavelength region. Therefore we made measurements at the actual angles of operation. Some parameters are listed in Table 1.

Figure 8 shows a series of measurements made at the points listed in the table. We made these measurements before making many of the upgrades mentioned in the previous section. Therefore, these are preliminary results with uncertainties ($2\sigma$) of 0.02 nm in wavelength and 2% in reflectivity. We are in the process of making the final measurements on this piece and two other sectors from test depositions.

## 4. Conclusions and future work

We have installed the world's largest EUV reflectometry chamber and made extensive tests on both the mechanical system and the optical system with the goal of meeting the requirements of metrology for commercial EUV lithography systems. We are in the process of making upgrades to meet these goals. A unique double-slit system will allow us to measure simultaneously the intensity of the incident radiation to better than 0.1% and the wavelength to better than 0.002 nm. We have determined that our incident spectral purity is excellent. Through the appropriate operating settings of SURF III we can virtually eliminate any higher orders from our monochromator, and we have measured a very small contribution of broadband scatter from the monochromator. We are making measurements to further quantify this contribution.

## Acknowledgments

We would like to thank Rob Vest and Chris Evans for helpful suggestions and Eberhard Spiller for providing samples, data, and advice.



Downloaded From: http://proceedings.spiedigitallibrary.org/ on 01/27/2016 Terms of Use: http://spiedigitallibrary.org/ss/TermsOfUse.aspx

## References

[1] C. Tarrio, R. N. Watts, T. B. Lucatorto, M. Haass, T. A. Callcott, and J. Jia, "New NIST/DARPA National Soft X-ray Reflectometry Facility," J. X-ray Sci. Tech. **4**, 96 (1994).
[2] E. Spiller, J. Wilczynski, L. Golub, G. Nystrom, E. Gullikson, and C. Tarrio, "Normal-Incidence Optics for Solar Coronal Imaging," Proc. SPIE **2515**, 136-144 (1995).
[3] D. L. Shealy, W. Jiang, and R. B. Hoover, "Design and analysis of aspherical multilayer imaging x-ray microscope," Opt. Eng. 30, 1094 (1991).
[4] D. Stutman, M. Finkenthal, V. Soukhanovskii, M. J. May, H. W. Moos, R. Kaita, "Ultrasoft x-ray imaging system for the National Spherical Torus Experiment," Rev. Sci. Instrum. **70**, 572 (1999).
[5] R. H. Stulen and D. W. Sweeney "Extreme Ultraviolet Lithography," *Optics and Photonics News*, August 1999, pp. 35-8.
[6] M. L. Furst, U. Arp, G. Cauchon, R. M. Graves, A. D. Hamilton, L. R. Hughey, T. B. Lucatorto, and C. Tarrio, "Selected programs at the new SURF III electron storage ring," AIP Conf. Proc. **561**, 87 (2000).
[7] E. M. Gullikson, S. Mrowka, and B. B. Kaufmann, "Recent Developments in EUV Reflectometery at the ALS", SPIE vol. 4343 (2001).
[8] M. L. Schattenburg , E. H. Anderson, and H. I. Smith, "X-ray/VUV transmission gratings for astrophysical and laboratory applications," Physica Scripta **41,** 13 (1990).



**Downloaded From: http://proceedings.spiedigitallibrary.org/ on 01/27/2016 Terms of Use: http://spiedigitallibrary.org/ss/TermsOfUse.aspx**